Successive metamagnetic transitions and magnetoresistance in the low-carrier-density strongly correlated electron system CeP

T. Terashima,* S. Uji, and H. Aoki
Tsukuba Magnet Laboratory, National Research Institute for Metals, Tsukuba, Ibaraki 305, Japan

J. A. A. J. Perenboom
Research Institute for Materials and High Field Magnet Laboratory, University of Nijmegen, NL-6525 ED, Nijmegen, The Netherlands

Y. Haga
Advanced Science Research Center, Japan Atomic Energy Research Institute, Tokai, Ibaraki 319-11, Japan

A. Uesawa and T. Suzuki
Department of Physics, Tohoku University, Sendai 980-77, Japan

S. Hill and J. S. Brooks
National High Magnetic Field Laboratory, Tallahassee, Florida 32310
(Received 12 December 1997)

Successive metamagnetic transitions in CeP are studied through magnetoresistance measurements up to 31.5 T over a wide temperature range between 0.7 and 44.1 K. As in previous papers, we find a series of transitions in field and temperature that constitute a phase diagram. However, we find the observed transitions not to be periodic in inverse field, and hence our results do not support previous models where the transitions are triggered by crossings of the up- and down-spin Landau levels in a particular electronic energy band. The present phase diagram reveals a close similarity to that of CeSb, and its general features are satisfactorily explained with a simple thermodynamic model. [S0163-1829(98)01425-8]

INTRODUCTION

The semimetallic cerium monopnictides CeX (X=P, As, Bi, and Sb) with the NaCl structure have been an object of extensive studies for many years.[1,2] The carrier concentration in these compounds is very low, a few %/Ce or less, and the strong interplay between the carriers and the Ce $4f$ spin system leads to highly unusual magnetic and transport properties such as the complex magnetic phase diagram of CeSb.[2] Compared with CeSb, the title compound CeP was thought to be rather conventional. However, recent detailed investigations of CeP, made possible by successful growth of high-quality single crystals, have revealed that CeP is as rich as CeSb in the anomalous physical properties.[3,4]

Figure 1 shows a schematic magnetic field versus temperature (H-T) phase diagram of CeP at low temperatures and low magnetic fields applied parallel to [001].[4] In the paramagnetic state, the crystal-field ground state of the Ce^{3+} ion is Γ_7 with the excited Γ_8 state about 150 K above.[5] At zero magnetic field CeP orders antiferromagnetically below T_N=10.5 K with a simple type-I structure. The ordered moment, which is parallel to the $\langle 001 \rangle$ axis, is 0.8 μ_B, close to the value expected for the Γ_7 ground state.[6] With the magnetic field applied, three distinct regions called phases I, II, and III appear in the phase diagram. Neutron-scattering experiments have shown that two kinds of the Ce spins coexist in these regions (Fig. 1): one is the Γ_7 spin with a magnetic moment of 0.7 μ_B, while the other is the Γ_8 spin with 2 μ_B.[6] The spin structure in phase I is an eleven layer one consisting of a ferromagnetically coupled double layer of the Γ_8 spins and antiferromagnetically coupled nine layers of the Γ_7 spins. The spins are ferromagnetically coupled within each layer. On entering phase II with increasing field, the Γ_7 spins are canted. In phase III, the Γ_7 spins are paramagnetic and the period of the spin structure observed at 5.3 T is ten layers.[6] It is an intriguing problem why the Γ_8 state is stabilized in these phases despite the large crystal-field separation. To answer this, Kasuya and co-workers argue formation of magnetic polarons based on the p-f mixing model.[7]

The most mysterious phenomenon found in CeP is successive metamagnetic transitions occurring at high magnetic fields above 20 T.[8] They were observed as steps in magnetization curves recorded with pulsed magnetic fields. The transition fields were reported to be equally spaced on the scale of the inverse field $(1/H)$. By analogy with the ordinary de Haas-van Alphen (dHvA) effect, the transition frequency F_{meta} may be defined from the spacing of the transitions as $F_{\mathrm{meta}}=[\Delta(1/H)]^{-1}$. For the field direction [001], F_{meta} agreed well with a frequency observed in early Shubnikov-de Haas (SdH) effect measurements. To explain the phenomenon, Kuroda *et al.* proposed the Stoner-Landau model, in which the metamagnetic transitions are triggered by crossings of up- and down-spin Landau levels in the particular electronic energy band whose Fermi surface was seen via the SdH oscillation.[8] In previous dHvA effect measurements below 14 T, we also confirmed that F_{meta} agrees well with one of the dHvA frequencies α_1, observed in phase II for all directions of the magnetic field.[9] However, our recent dHvA effect measurements up to 20 T cast some doubt about such correlation between the metamagnetic transitions and

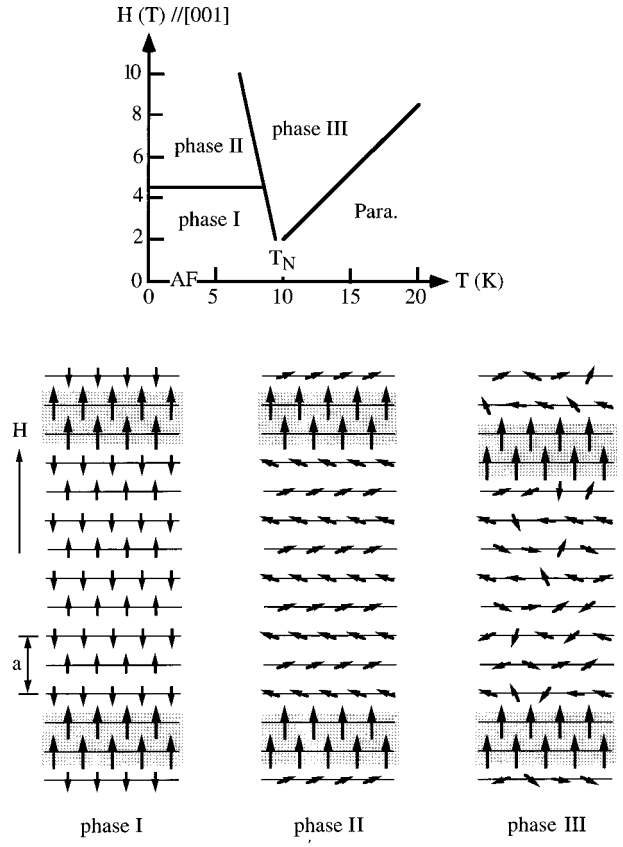

FIG. 1. Simplified magnetic phase diagram for magnetic fields below 10 T applied parallel to the [001] axis of CeP (based on Ref. 4) and spin structures determined by neutron-scattering experiments (Ref. 6). The long and short arrows indicate the Γ_8 and Γ_7 spins, respectively.

the Fermi surface. In a higher-field phase than phase II, the α_1 frequency corresponding to F_{meta} can be detected only for limited field directions around [001].[10] If the α_1 frequency were directly connected with the successive metamagnetic transitions, it should be observed for all field directions.

In this work, we have studied the successive metamagnetic transitions through magnetoresistance measurements up to 31.5 T over a wide temperature range. The phase diagram thus obtained shows appreciable disagreement at low temperatures with that of a previous work based on pulsed-field magnetization measurements. Our data do not favor a correlation between the successive metamagnetic transitions and the Landau quantization of the conduction-electron energy: the positions of the transition fields are not equally spaced on the $1/H$ scale. Rather, the data clearly indicate a close relation between the successive metamagnetic transitions in CeP and the ferroparamagnetic (FP) phase of CeSb (Ref. 2).

EXPERIMENTAL PROCEDURES AND RESULTS

The single crystal of CeP used in this study was grown by a recrystallization method as described in Ref. 3. The magnetoresistance in magnetic fields up to 31.5 T was measured between 0.7 and 44.1 K with the standard four contact method using an ac current ($f=100$ Hz). The magnetic field was applied in the [001] direction and was parallel to the current (longitudinal configuration). For magnetic field ramping, a slow sweep rate of about 0.04 T/s was normally used to minimize the eddy current heating. The sample and a Cernox resistance thermometer were mounted as closely as possible on the same copper plate to eliminate temperature differences between them. Temperature control below 4 K was done by stabilizing ^{4}He or ^{3}He pressure, while above 4 K a heater was employed using a PID temperature controller with the Cernox thermometer. In the latter case, the temperature error due to the magnetoresistance of the sensor is estimated to be a few % between 4 and 15 K, and less than 1% above 15 K.[11] To avoid complications due to magnetic hysteresis, the magnetoresistance measurements below T_N were always made after heating the sample above T_N and cooling it in zero magnetic field.

We show the magnetoresistance at 0.7 K in Fig. 2(a) as a typical magnetoresistance trace observed below T_N. With increasing field, the resistivity starts to increase sharply at about 0.3 T, reaches the maximum at $H_p=0.9$ T, and then decreases. Small features appear at 2.4 and 3.6 T. The resistivity drops further at $H_f=4.6$ T and $H_c=14.5$ T. The oscillations in the resistivity between H_f and H_c are due to the SdH effect. No clear transition appears above H_c. However, apparent hysteresis is observed between the up- and down-field-sweep traces. The single H_f transition in the up-sweep trace splits into two successive transitions, H_f at 4.6 T and $H_{f'}$ at 3.6 T, in the down-sweep trace. The resistivity peak does not appear in the down-sweep trace.

Figure 2(b) shows the magnetoresistance at $T=23.3$ K ($>T_N$). On entering the phase III region at the magnetic field H_0, the resistivity decreases sharply. Above H_0, five distinct transitions from H_1 to H_5, all accompanied by a resistivity decrease, appear with a broad hysteresis. They correspond to the successive metamagnetic transitions observed in the magnetization. Figure 2(c) shows the magnetoresistance traces as a function of temperature above T_N. (Note that we used a higher sweep rate to record the $T=44.1$ K trace. Therefore, the hysteresis in the $T=44.1$ K trace, which appears to persist to very low fields, is most likely due to a time delay caused by the time constant of a lock-in amplifier.) With increasing temperature, the transition field H_0 increases rapidly and the accompanying resistivity decrease becomes less sharp. It seems that the H_0 transition changes from first order to second order at about 40 K. At low temperatures, the hysteresis of the successive metamagnetic transitions H_1–H_5 are remarkably large, extending for more than 5 T for the H_5 transition at 11.0 K. The hysteresis becomes smaller with increasing temperature, but is still prominent even at $T=39.5$ K. The transition fields show a clear but nonmonotonic temperature variation: they first shift to higher fields, reach a maxima at about 30 K, then decrease.

Because of the temperature dependence of the successive metamagnetic transitions, the transitions are also visible in temperature variation of the resistivity at a constant field. In the $H=23$ T resistivity trace shown in the inset of Fig. 2(a), the broad hysteresis extending between about 20 and 28 K is due to the H_4 transition.

Figure 3 summarizes all the transitions and anomalies observed in the resistivity versus magnetic-field traces. Note that all the transitions H_0–H_5, except H_0 above about 40 K, are of first order judging from their apparent hysteresis. The

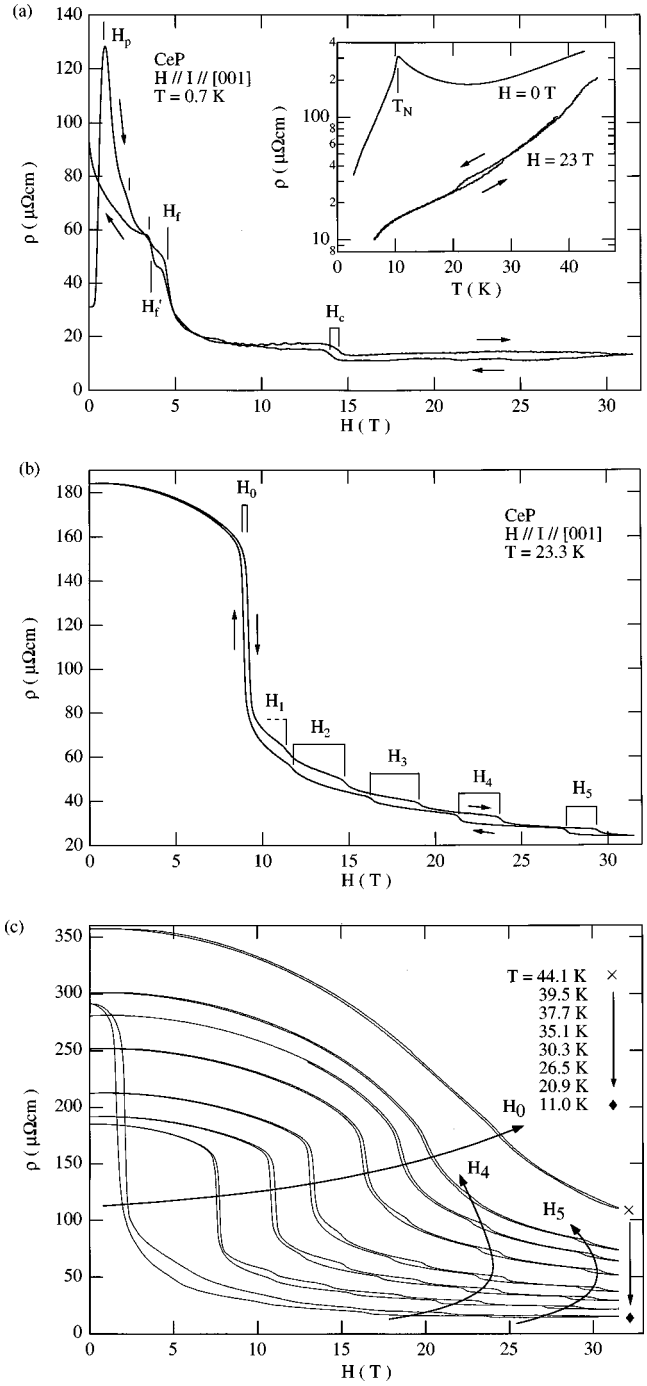

FIG. 2. Resistivity of CeP as a function of the magnetic field at (a) $T=0.7$ K, (b) $T=23.3$ K, and (c) several temperatures above $T_N=10.5$ K. The magnetic field and the electric current were parallel and applied along the [001] direction. The curves H_0, H_4, and H_5 shown in the figure (c) are guides to the eye. The inset of the figure (a) shows temperature dependence of the resistivity at constant fields.

transitions, I, II, D, E, F, and j, reported by Kuroda *et al.* are also shown by dotted lines.[8] Our H_0 transition most likely corresponds to the transition I, though two branches diverging from the phase boundary I, the transition II, and the other one starting at about 34 K, were not observed in the present study. Our H_2, H_3, H_4, and H_5 transitions seem to correspond to the transitions j, F, E, and D, respectively.

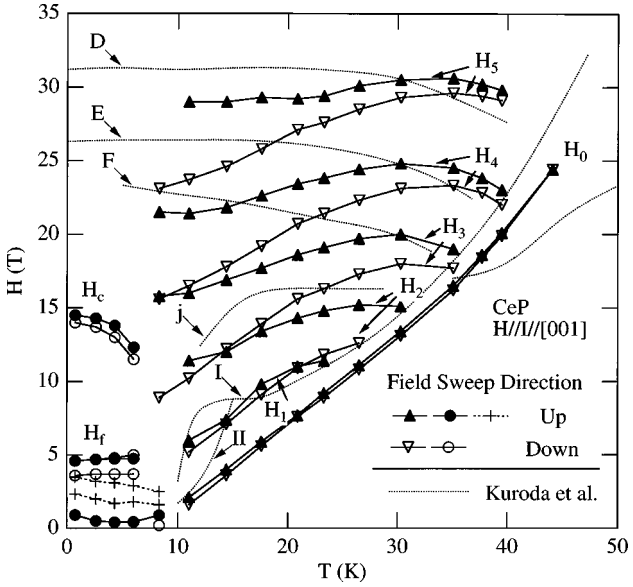

FIG. 3. Transition fields determined from resistivity vs magnetic field traces. The closed symbols and crosses indicate the up-sweep data, while the open symbols show the down-sweep data. The transition fields determined by Kuroda *et al.* (Ref. 8) are shown by dotted lines for comparison.

Figure 4 shows the inverse transition fields $1/H_1-1/H_5$ at 11.0 K against an integer index (with arbitrary zero). Since the hysteresis is large, we have plotted not only the up- and down-sweep data but also their medians, which are expected to be good approximation to the thermodynamic transition fields. The transitions $A-F$ reported by Kuroda *et al.* are also shown for comparison (they observed three transitions A, B, and C above the transition D).[8] Clearly, our data do not lie on a straight line, and do not support the inverse field relationship.

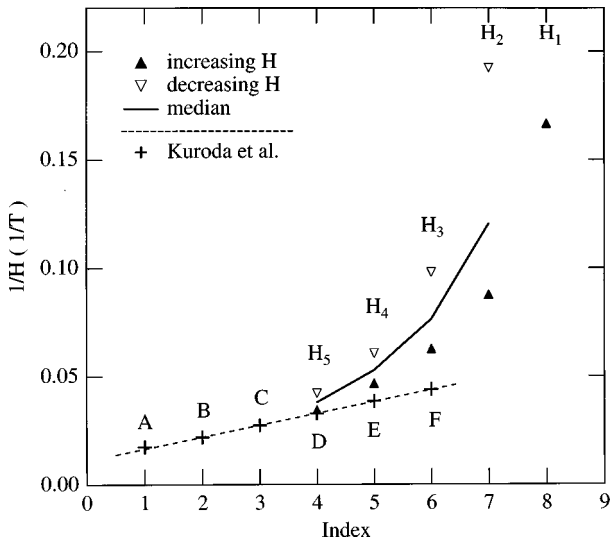

FIG. 4. Inverses transition fields, $1/H_0-1/H_5$, at 11 K against an integer index (with arbitrary zero). The closed (open) triangles indicate the up-field-sweep (down-field-sweep) data. The solid line shows the medians of the up- and down-sweep transition fields. The inverses transition fields, $1/A-1/F$, determined by Kuroda *et al.* (Ref. 8) are also shown for comparison.

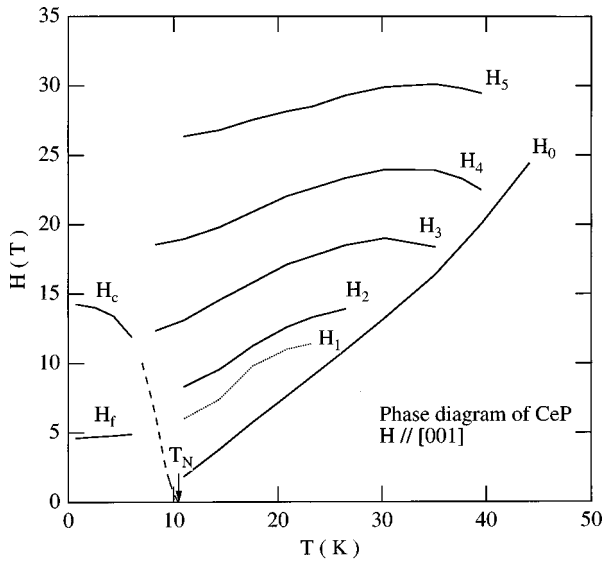

FIG. 5. Magnetic phase diagram of CeP for the magnetic field parallel to the [001] axis based on the medians of the up- and down-field-sweep transition fields. Since the H_1 transition is not observed in a down sweep, the up-sweep transitions are shown by the dotted line. The broken line determined from low-field magnetization is reproduced from Ref. 12.

Figure 5 shows the H-T phase diagram based on the medians of the up- and down-sweep transition fields. Since the H_1 transition is not observed in the down sweeps, the up-sweep data are shown by a dotted line. Some transitions or anomalies are omitted for simplicity. The broken line determined from low-field magnetization data is reproduced from Ref. 12.

DISCUSSION

The discrepancy between the data of Kuroda *et al.* (Ref. 8) and ours is appreciable, especially at low temperatures (Fig. 3). We note that Kuroda *et al.* determined the transition fields based only on up sweeps of the pulsed-magnetic field. Since their transition lines deviate upward from ours at low temperatures, part of the discrepancy is attributed to the difference in sweep rates of the magnetic field. It is possible that the rise of the pulsed magnetic field is too fast compared with the magnetic relaxation of the sample. Another noticeable discrepancy is that we did not see well-developed transitions above H_c below T_N where Kuroda *et al.* observed the transitions D and E. This point will be discussed later. The most important manifestation of the discrepancy is that the inverses of our transition fields are not equally spaced (Fig. 4). Therefore, our data do not support the idea that the successive metamagnetic transitions are directly connected with the crossing of up- and down-spin Landau levels in a specific conduction-electron energy band.

The magnetoresistance traces observed below T_N [Fig. 2(a)] are compatible with previous works on magnetization, ac susceptibility, dHvA effect, and neutron scattering. The magnetization data at 4.2 K indicate that the transition from the zero-field antiferromagnetic (AF) state to phase I is accompanied by a gradual increase in the magnetization between about 0.1 and 1 T rather than a sharp jump.[12] The initial steep increase in the resistivity is probably due to disorder introduced by random nucleation of phase I domains. The peak field H_p may thus be assigned to the field where the gradual transformation finishes. Then the domains merge into larger ones and the magnetic ordering becomes more perfect. This could be an origin of the subsequent decrease in the resistivity. The magnetization data also indicate that, after application of the magnetic field, phase I instead of the AF state stays stable in zero-magnetic field.[12] Thus the lack of the resistivity peak in the down-sweep trace is also in line with the magnetization data. The H_f transition is attributed to the spin-flop transition in the AF Γ_7 layers as was demonstrated by the neutron-scattering experiments.[6] Then the H_c transition can be ascribed to the transition to the field-induced ferromagnetic state of the Γ_7 layers. The ac susceptibility data support the interpretation (Ref. 10): it drops at the H_c transition as is usually observed in an antiferromagnet when a field-induced ferromagnetic state is stabilized over a spin-flop state with increasing field. The most remarkable feature in Fig. 2(a) is the fact that the up- and down-sweep traces never coincide with each other. This is in accord with unusually history-sensitive dHvA oscillations reported previously.[9] The dHvA oscillations in an up sweep of the field and those in a subsequent down sweep were found to be very different.

The absence of the transitions H_1–H_5 below T_N in our data can be justified by taking account of the extraordinarily strong hysteresis. The strong hysteresis implies substantial energy barriers between different magnetic phases. Since there is a definite difference between the up-sweep and down-sweep traces of the magnetoresistance above H_c [Fig. 2(a)], it is apparent that different magnetic phases are nucleated above H_c even below T_N. However, because of the large energy barrier, the local nucleation of a magnetic phase can not develop into a full phase transition over the whole crystal. That is, the transitions are smeared out by the hysteresis. The ac susceptibility data provide indications of such nucleations. Several sharp spikes have been recorded in low-temperature ($T=0.05$ K) ac susceptibility measurements.[10] The fields where the spikes appear differ each time. They could be due to the local nucleation of magnetic phases. The question why Kuroda *et al.* observed the successive transitions even below T_N remains to be answered. One possible explanation could be sample heating due to the quick rise of the pulsed field.

The phase boundaries H_1–H_5 in the present phase diagram (Fig. 5) quite resembles the phase boundaries between FP phases of CeSb (Ref. 2). The magnetic structure in the FP phases is characterized by regular stacking of ferromagnetic and paramagnetic layers. With increasing field, stacking sequences with a denser ferromagnetic-layer content appear in order. The phase boundaries between those phases are approximately parallel in the H-T plane. In the case of CeP, a regular lattice of the ferromagnetic Γ_8 layers forms in the sea of the paramagnetic Γ_7 layers above H_0 (the phase III region). By analogy to the CeSb FP phases, we assume that the transitions H_1–H_5 correspond to discontinuous increases in the Γ_8 to Γ_7 ratio. Then general features of the phase boundaries H_0–H_5 are well explained by a simple thermodynamic model that is essentially the same that applied by Rossat-Mignod *et al.* to explain the complex phase diagram of

CeSb.[2] We attribute given magnetic moment M_7 (M_8) and entropy S_7 (S_8) to a Γ_7 (Γ_8) spin. The slopes of the phase boundaries are determined by the formula $dH/dT = -\Delta S/\Delta M$, where $\Delta S = S_8 - S_7$ and $\Delta M = M_8 - M_7$. Letting $S_7 = k \ln 2$ and $M_7 = 0$ since the Γ_7 spins are paramagnetic, and letting $S_8 = 0$ and $M_8 = 2\mu_B$ since the Γ_8 spins are ferromagnetically ordered, we have $dH/dT = 0.59$ T/K, which is close to the observed slope of the H_0 transition, 0.52 T/K in the limit of $H \rightarrow 0$. This simplified model predicts the same slope for all the phase boundaries H_0–H_5, while the slopes of the observed phase boundaries become smaller at higher fields. This is because ΔS becomes zero before ΔM: ΔM stays finite even when the Γ_7 spins are fully aligned by the magnetic field and hence $S_7 = 0$. One important feature that the model fails to explain is the negative slopes of H_3, H_4, and H_5 above about 30 K. The local maxima of the phase boundary lines indicate that the entropies of the Γ_8 and Γ_7 spins are comparable at this temperature regime. We may ascribe this to excitations within the Γ_8 state that may no longer be negligible. A quantitative argument is, however, not possible until the stabilization mechanism of the Γ_8 state is clarified.

Since the H-T and pressure versus temperature phase diagrams of CeP are known to be very similar,[4] it is interesting to note results of high-pressure neutron-scattering experiments. The magnetic structures 9°, 8°, 7°, and so on appear in order with increasing pressure,[13] where the structure $n°$ has an n-layer period composed of a ferromagnetic Γ_8 double layer and $(n-2)$ paramagnetic Γ_7 layers. If we apply the same scenario to the H-T phase diagram, the magnetic structure just above H_5 will be 5° (note that the magnetic structure just above H_0 is 10°). According to the pulsed-field magnetization measurements, three or four transitions are expected above H_5 and they are enough to drive the whole spin system into a complete ferromagnetic state (the magnetic structure 2°), though one extra spin structure other than the $n°$ series is necessary in the case of the four transitions.

CONCLUSION

The successive metamagnetic transitions in CeP were clearly observed in the resistivity versus magnetic field and resistivity versus temperature traces. The phase diagram obtained shows considerable disagreement with one previously determined from magnetization measurements in pulsed magnetic fields. The present transition fields are not equally spaced on the $1/H$ scale, thereby giving strong evidence against the idea that the metamagnetic transitions are directly connected with the Landau-quantization of a specific conduction-electron energy band. The present phase diagram reveals a close relation to the FP phases of CeSb. We can account for the general features of the phase diagram using the simple thermodynamic model that is essentially the same as previously applied to CeSb. We have speculated that the magnetic structure will change from 10° to 9°, 8°, and so on with increasing magnetic field. It would be very interesting that such changes are confirmed by neutron-scattering experiments in pulsed magnetic fields. The local maxima of the phase boundary lines appearing around 30 K at high fields are worthy of further investigations in relation to the magnetic polaron model of CeP. It could provide valuable information about how the magnetic polaron evolves with the temperature.

*Present address: National High Magnetic Field Laboratory, Tallahassee, Florida 32310 (on leave from NRIM).

[1] T. Kasuya, O. Sakai, J. Tanaka, H. Kitazawa, and T. Suzuki, J. Magn. Magn. Mater. **63&64**, 9 (1987).

[2] J. Rossat-Mignod, P. Burlet, J. Villain, H. Bartholin, Wang Tcheng-Si, D. Florence, and O. Vogt, Phys. Rev. B **16**, 440 (1977); J. Rossat-Mignod, J. M. Effantin, P. Burlet, T. Chattopadhyay, L. P. Regnault, H. Bartholin, C. Vettier, O. Vogt, D. Ravot, and J. C. Achart, J. Magn. Magn. Mater. **52**, 111 (1985).

[3] Y. S. Kwon, Y. Haga, O. Nakamura, T. Suzuki, and T. Kasuya, Physica B **171**, 324 (1990).

[4] For a review, see, T. Suzuki *et al.*, Physica B **206&207**, 771 (1995).

[5] M. Kohgi, Y. Osakabe, N. Môri, H. Takahashi, Y. Okayama, H. Yoshizawa, Y. Ohara, S. Ikeda, T. Suzuki, and Y. Haga, Physica B **186-188**, 393 (1993).

[6] M. Kohgi, T. Osakabe, K. Kakurai, T. Suzuki, Y. Haga, and T. Kasuya, Phys. Rev. B **49**, 7068 (1994); M. Kohgi, T. Osakabe, T. Suzuki, Y. Haga, T. Kasuya, and Y. Morii, Physica B **206&207**, 783 (1995).

[7] T. Kasuya, T. Suzuki, and Y. Haga, J. Phys. Soc. Jpn. **62**, 2549 (1993); T. Kasuya, Y. Haga, T. Suzuki, T. Osakabe, and M. Kohgi, *ibid.* **62**, 3376 (1993).

[8] T. Kuroda, K. Sugiyama, Y. Haga, T. Suzuki, A. Yamagishi, and M. Date, Physica B **186-188**, 396 (1993); T. Inoue, T. Kuroda, K. Sugiyama, Y. Haga, T. Suzuki, and M. Date, J. Phys. Soc. Jpn. **64**, 572 (1995).

[9] T. Terashima, S. Uji, H. Aoki, W. Joss, Y. Haga, A. Uesawa, and T. Suzuki, Phys. Rev. B **55**, 4197 (1997).

[10] T. Terashima, C. Haworth, M. Takashita, S. Uji, H. Aoki, Y. Haga, A. Uesawa, and T. Suzuki, J. Magn. Magn. Mater. **177-181**, 421 (1998).

[11] B. L. Brandt and D. W. Liu, Rev. Sci. Instrum. (to be published).

[12] Y. Haga, Ph.D. thesis, Tohoku University (1994); T. Suzuki, in *Physical Properties of Actinide and Rare Earth Compounds*, JJAP series 8, edited by T. Kasuya, T. Ishii, T. Komatsubara, O. Sakai, N. Mori, and T. Saso (Jpn. J. Appl. Physics, Tokyo, 1993), p. 267.

[13] T. Osakabe, M. Kohgi, K. Iwasa, N. Nakajima, J. M. Mignot, I. N. Goncharenko, Y. Okayama, H. Takahashi, N. Môri, Y. Haga, and T. Suzuki, Physica B **230-232**, 645 (1997).